Chem-Bio Informatics Journal, Vol.18, pp.44-57 (2018)

Binding properties between curcumin and malarial tubulin: molecular-docking and *ab initio* fragment molecular orbital calculations

Shintaro Ota[1], Shougo Tomioka[1], Haruki Sogawa[1], Riku Satou[1], Mitsuki Fujimori[1], Pavel Karpov[2], Sergey Shulga[2], Yaroslav Blume[2], Noriyuki Kurita[1]*

[1]*Department of Computer Science and Engineering, Toyohashi University of Technology, Tempaku-cho, Toyohashi, Aichi, 441-8580, Japan*
[2]*Institute of Food Biotechnology and Genomics, National Academy of Sciences of Ukraine, 2a, Osypovskogo str., Kyiv-123, 04123, Ukraine*

**E-mail: kurita@cs.tut.ac.jp*

(Received December 22, 2017; accepted March 12; published online March 25, 2018)

Abstract

Curcumin can bind to tubulin and inhibit the formation of tubulin polymer, which contributes to the formation of microtubule. Binding sites of curcumin on the α- and β-tubulin heterodimer were predicted by a molecular docking study to ascertain probable causes for the observed anti-microtubule effects of curcumin. However, the specific interactions between curcumin and the tubulins have yet to be elucidated at an electronic level. We here investigated the binding properties between curcumin and α- or β-tubulin of *Plasmodium falciparum*, using *ab initio* fragment molecular orbital (FMO) calculations, in order to reveal the preferable binding sites of curcumin on these tubulins. The results were compared with those for some microtubule destabilizing drugs evaluated by the same method to confirm the efficiency of curcumin as an inhibitor to the tubulins. Our *ab initio* FMO calculations might provide useful information for proposing novel therapeutic agents with significant binding affinity to both the α- and β-tubulins.

Key Words: Curcumin, Tubulin, Microtubule, Malaria parasite, Drug resistance, Inhibitor, Fragment molecular orbital, Protein ligand interaction, Molecular docking

Area of Interest: *In silico* drug discovery

1. Introduction

Malaria is a life-threatening disease caused by malaria parasites, and it infects human beings via the biting of female anopheles holding the parasites. In particular, children under 5 years old are prone to be infected by this disease, causing a large number of deceased children. There are five types of parasites causing malaria in human beings. Among them, *Plasmodium falciparum* and *Plasmodium vivax* can pose a serious danger to human life. According to the WHO report [1] released in 2016, 216 million malaria patients and 445 thousand malaria deaths were estimated in 2016.

In the treatment for malaria, the drug resistance of malaria parasites is a serious problem that needs to be solved. For example, in the 1970s and 1980s, malaria parasites with resistance against the previous-generation drugs such as chloroquine and sulfadoxine-pyrimethamine spread worldwide to cause the death of many children. Recently, combination drug therapy has been applied for the treatment of malaria patients. However, drug-resistant malaria parasites against the concurrent drug artemisinin have appeared in the countries of the Greater Mekong Subregion [1]. In Cambodia and Thailand, falciparum malaria parasites with a multi-drug resistance against both artemisinin and its concomitant drugs have appeared and spread [1]. Therefore, it is indispensable to develop novel medicines that do not engender drug-resistance in malaria parasites.

Curcumin, a naturally occurring phenolic derivative, has been used widely as a traditional medicine [2]. Previous experiments [3-5] revealed that curcumin possess anti-malarial activity against various plasmodia of malaria. Curcumin was also demonstrated to down-regulate the gene expression for producing tubulins in cancer cells [6]. Tubulins play an important role in cell division and cellular transport. It was proven that curcumin can bind tubulin and inhibit the formation of α/β-tubulin heterodimers [7]. The effect of curcumin on the organization of *Plasmodium falciparum* microtubules in cultured parasites was investigated by immunofluorescence studies [8], and the binding sites of curcumin on the α- and β-tubulin heterodimer were predicted by a molecular docking study, in order to ascertain probable causes for the observed anti-microtubule effects of curcumin [8]. However, the specific interactions between curcumin and the tubulins have not been elucidated at the atomic and electronic levels.

In the present study, we investigated the binding properties between curcumin and the α- or β-tubulin, using *ab initio* fragment molecular orbital (FMO) calculations, in order to reveal the preferable binding sites of curcumin on the α- as well as β-tubulins of *Plasmodium falciparum*. In addition, the binding properties of the microtubule destabilizing medicines such as vinblastine [9] and colchicine [10] were investigated in the same way, and the results were compared with those for curcumin, in order to confirm the efficiency of curcumin as an inhibitor for the tubulins. Our present results obtained by the *ab initio* FMO calculations might be useful for proposing novel therapeutic agents with significant binding affinity to the α- and β-tubulins, which contribute greatly to the formation of microtubule.

2. Details of *ab initio* molecular simulations

In the present study, the amino acid sequences of malaria α- and β-tubulins were taken from the universal protein resource UniProtKB (http://www.uniprot.org/), and the three-dimensional structure models for these tubulins were built using a protein modelling server I-TASSER (Iterative Threading Assembly Refinement) [11][12], because there is no crystal structure of tubulins for

Plasmodium falciparum. The UniProt ID is P14642 for the α-tubulin and P14140 for the β-tubulin, respectively. The N- and C-termini of the tubulins were terminated by the acetyl group and the amine group, respectively, to make the charge of both terminal groups zero. The malaria α- and β-tubulins have 11 and 10 His residues, respectively, and their protonation states were assigned based on the pKa value predicted by PROPKA3.1 program [13][14]. The His residues with a pKa value larger than six were assigned as Hip^+ protonation, while the other His residues were assigned as Hid protonation.

As the ligands for tubulins, we here employed the keto-form of curcumin-I and the microtubule destabilizing medicines vinblastine and colchicine. Their chemical structures are shown in Figure 1, and their three-dimensional structures were optimized using the B3LYP/6-31G(d,p) method of the *ab initio* molecular orbital (MO) calculation program Gaussian09 (G09) [15]. To obtain the charge parameters used in the molecular mechanics (MM) force field for these ligands, the charge distributions of the optimized structures were evaluated by RESP (Restrained Electrostatic Potential) [16] analysis using the HF/6-31G(d) method of G09. It is noted that these charge distributions were used in the docking simulations as well as the MM optimizations, in order to accurately describe the electrostatic interactions between the tubulin and these ligands.

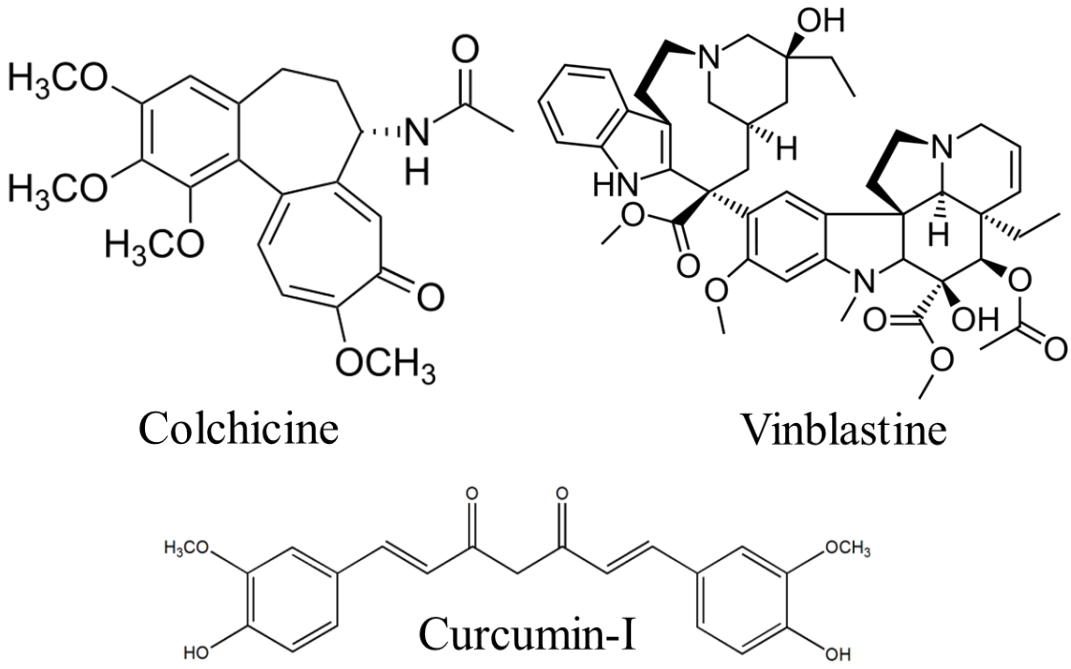

Figure 1. Chemical structures of ligands employed in the present study

The initial structures for the tubulin+colchicine and tubulin+vinblastine complexes were obtained by fitting the tubulin structure created by I-TASSER to that registered in PDB, using Swiss-PDB Viewer Ver.4.1.0 (https://spdbv.vital-it.ch/). The PDB structures of tubulin+colchicine (PDB ID: 4O2B) and tubulin+vinblastine (PDB ID: 4EB6) were employed for the fitting. It is noted that colchicine and vinblastine bind to the different sites of α- and β-tubulins, and that the amino-acid sequence homology of the ligand-binding pocket is significantly different. On the other hand, since there is no structure registered in PDB for the tubulin+curcumin-I complex, we here used the protein-ligand docking program AutoDock4.2 [17] for creating candidate structures of the docked curcumin-I to the tubulin. In the docking simulations, we set the center of the grid box as

the center of the ligand (colchicine or vinblastine) in the PDB structures of the complexes of tubulin with the ligand. The size of the grid box was set as 30×30×30 $Å^3$. In the docking simulations, the tubulin structure was fixed, while all rotatable bonds in curcumin-I were free to rotate, in order to obtain various poses for the docked curcumin-I. The number of candidate poses created was 250, and the threshold distance for clustering these poses was set as 2 Å, in order to search in detail for the preferable docking sites of curcumin-I.

To obtain stable structures of the tubulin+ligand complexes, some candidate structures obtained by the docking simulations were fully optimized in water, by use of the classical MM method. In the optimizations, the water molecules existing within 8 Å from the surface of the complex were considered explicitly, to properly describe the solvation effect on the complex. The MM and molecular dynamics simulation program AMBER12 [18] was used. The AMBERFF99-SBLIN force field [19], the TIP3P model [20] and the general AMBER force field (GAFF) [21] were used for tubulin, water molecules and ligand, respectively. The initial placement of water molecules were determined based on the TIP3P model, and the threshold value of energy gradient for the convergence in the MM optimization was set as 0.001 kcal/mol/Å.

To elucidate the specific interactions and binding affinity between tubulin and ligand, we investigated the electronic properties of the tubulin+ligand complexes in explicit waters, using the *ab initio* FMO method [22]. This method was developed as a method to enable electronic state calculations for large molecules [22], and it has been applied to many biomolecules to obtain accurate results comparable to experiments [23]. The target molecule is divided into units called fragments, and the electronic states of each fragment and fragment pair are calculated to obtain the total energy and total electron density of the entire molecule. Since the electronic states are calculated for the fragment pairs, the interactions between the fragments can be analyzed based on the FMO result. In the FMO calculation, the electronic state of each fragment is independently calculated, leading to a high parallelization efficiency of calculation. Accordingly, when a large-scale parallel computer is used, the FMO calculation time can be greatly shortened.

From the candidate structures of tubulin+curcumin-I complex obtained by the molecular docking and the MM optimization, the representative structures of the top three clusters, which included more than 10 candidate poses, were selected. In order to determine the most stable structure among these candidate ones, we accurately evaluated their total energies (TEs) by use of the *ab initio* FMO calculation program ABINIT-MP Ver.6.0 [24]. In the FMO calculations, water molecules existing within 10 Å from the ligand in the tubulin+ligand complex were considered explicitly, in order to accurately describe the effect of these water molecules on the specific interactions between tubulin and ligand. In the FMO calculations, MP2 [25][26] method, which can analyze π-π stacking, NH-π, CH-π interactions with high accuracy, and the 6-31G basis-set were used. Each amino acid residue of tubulin, ligand and each water molecule were assigned to a fragment in the present FMO calculations, because this fragmentation enables to analyze the interactions between each of the tubulin residues and ligand affected by the solvating water molecules. To highlight the important tubulin residues for the ligand binding, we analyzed the inter fragment interaction energies (IFIE) [23] obtained by the FMO calculations. In addition, to predict the binding affinity between tubulin and ligand, the binding energy (BE) between tubulin and ligand was estimated from the total energies (TEs) of the component structures using the following equation.

$$BE = -TE(\text{tubulin+ligand+water}) + TE(\text{tubulin+water}) + TE(\text{ligand+water}) - TE(\text{water}).$$

3. Results and discussion

3.1. Specific interactions between tubulin and existing drugs vinblastine and colchicine

To check the adequacy of the present molecular simulations, we first investigated the specific interactions between tubulin and the existing drugs vinblastine and colchicine and compared the simulated results with those obtained by the previous experiments [9][10].

We first investigated the interactions between α-tubulin and vinblastine. According to the results of our calculations, as shown in Figure 2(a), vinblastine interacts most strongly with Asn329, and it also interacts with Pro325. The interacting between vinblastine and these residues is shown in Figure 3(a). It was revealed that vinblastine can form two hydrogen bonds with Asn329. In addition, the oxygen atom of vinblastine electrostatically interacts with Pro325, while there is no significant interaction between vinblastine and the other residues. The Asn329 of α-tubulin was found to interact strongly with vinblastine in the experiment [27]. Therefore, our present results are comparable to that obtained by the experiment.

The IFIEs between the amino acid residues of β-tubulin and vinblastine were shown in Figure 4(a). Vinblastine interacts specifically with Thr221 and Thr219 of β-tubulin. As shown in Figure 3(b), vinblastine forms a hydrogen-bond with the CO group of the backbone between Pro220 and Thr221 and can interact electrostatically with Thr219. In the PDB structure (PDB ID: 4EB6 [27]), there is no data for residues numbered as 45th and 46th in the sequence of amino acid residues, and Pro222 interacts strongly with vinblastine. This Pro222 corresponds to Pro220 in our structure with a complete sequence of residues. Therefore, the structure model shown in Figure 3(b) is comparable to the results of the experiment [27].

Next, we investigated binding between colchicine and α-tubulin, using the FMO calculation. The IFIEs between colchicine and the α-tubulin residues are shown in Figure 5(a), which indicates that colchicine interacts most strongly with Ala180, and it additionally interacts with Thr179. The interacting structure between colchicine and these residues is shown in Figure 6(a). It was predicted that colchicine can form a hydrogen bond with the CO group of the backbone between Thr179 and Ala180 and interact electrostatically with Thr179. In the PDB structure (PDB ID: 4O2B [28]), Thr179 of α-tubulin was found to contribute to the interaction with colchicine. Consequently, our present results shown in Figures 5(a) and 6(a) are comparable with the experiment [28].

The IFIEs between β-tubulin and colchicine evaluated by FMO are shown in Figure 7(a). According to the results of calculations, colchicine interacts strongly with Lys350, Asn247 and Leu250 residues of β-tubulin. The interacting structure for these residues is shown in Figure 8(a), which indicates that colchicine can form a hydrogen bond with Lys350 and Asn247 and interacts electrostatically with Leu250. In addition, Cys314 exists near colchicine to interact with colchicine at several points, although its IFIE with colchicine is not so large. In the PDB structure (PDB ID: 4O2B [28]), there is not residues numbered as 43th and 44th in the sequence of amino acid residues for β-tubulin, and Leu248 and Asn249 were found to interact with colchicine. These residues correspond to Leu246 and Asn247 in our structure with a complete sequence of residues. Therefore, the structure shown in Figure 8(a) can explain the result of the experiment [28].

As mentioned above, it was confirmed that the present FMO calculations for the existing drugs (vinblastine and colchicine) provide their interacting properties with the α- and β-tubulins, which are comparable with the results obtained by the experiments [27][28].

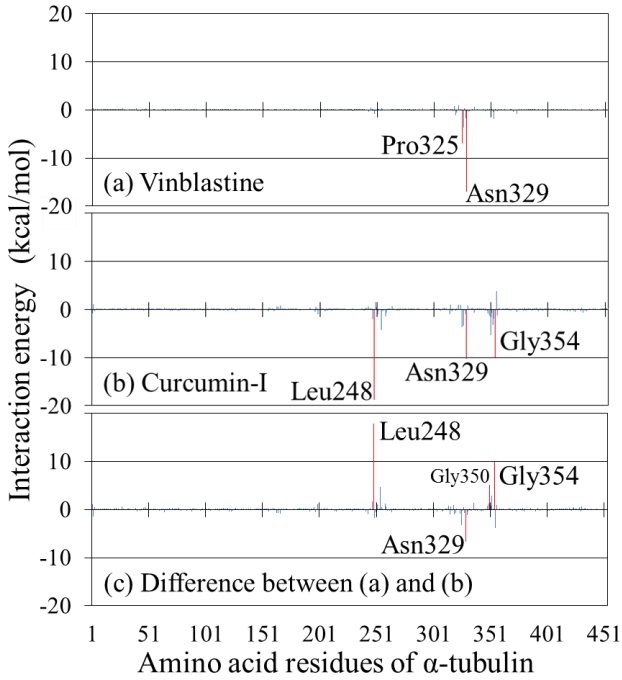

Figure 2. Interaction energies between amino acid residues of α-tubulin and ligand; (a) vinblastine, (b) curcumin-I and (c) difference between (a) and (b)
Curcumin-I is docked to the vinblastine-binding site of α-tubulin.

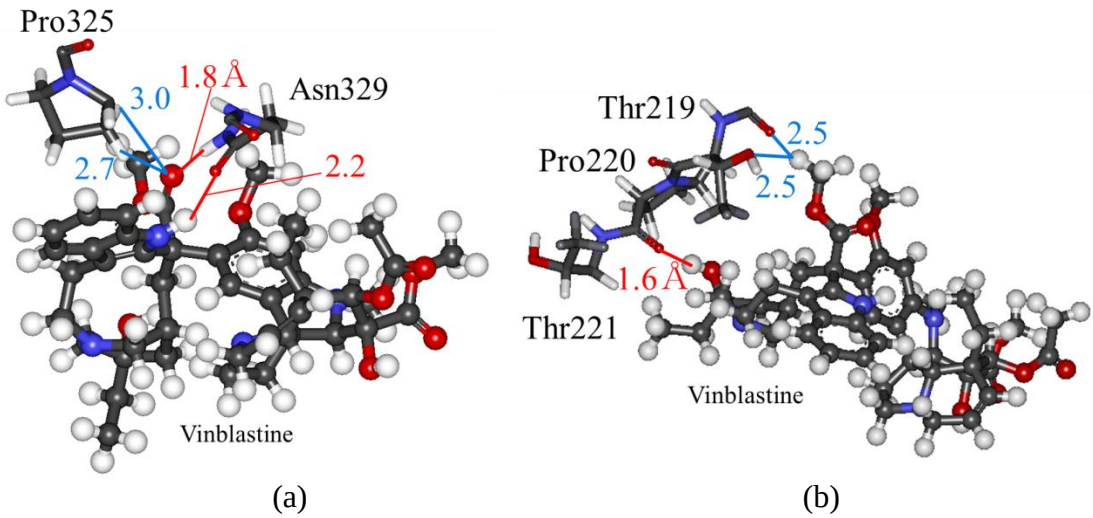

(a) (b)

Figure 3. Interacting structures between vinblastine and some residues of tubulin; (a) α-tubulin and (b) β-tubulin at the vinblastine binding-site
Red and blue lines indicate hydrogen-bonding and electrostatic interactions, respectively.

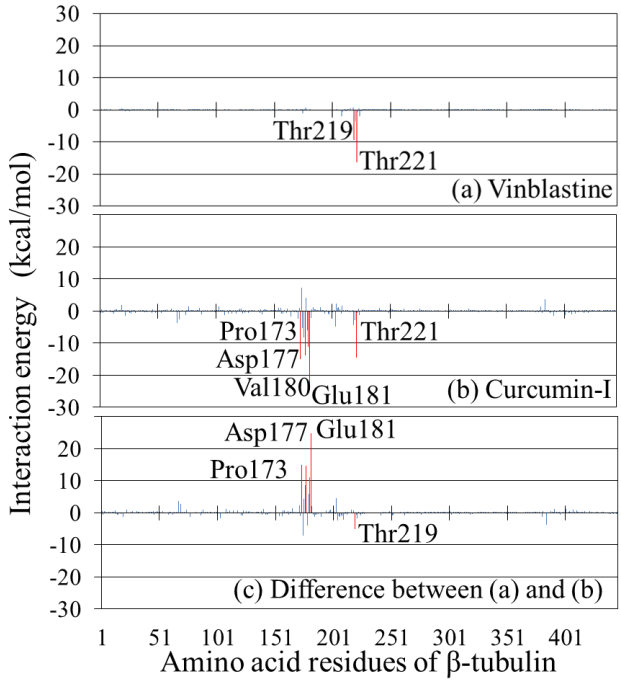

Figure 4. Interaction energies between amino acid residues of β-tubulin and ligand; (a) vinblastine, (b) curcumin-I and (c) difference between (a) and (b)
Curcumin-I is docked to the vinblastine site of β-tubulin.

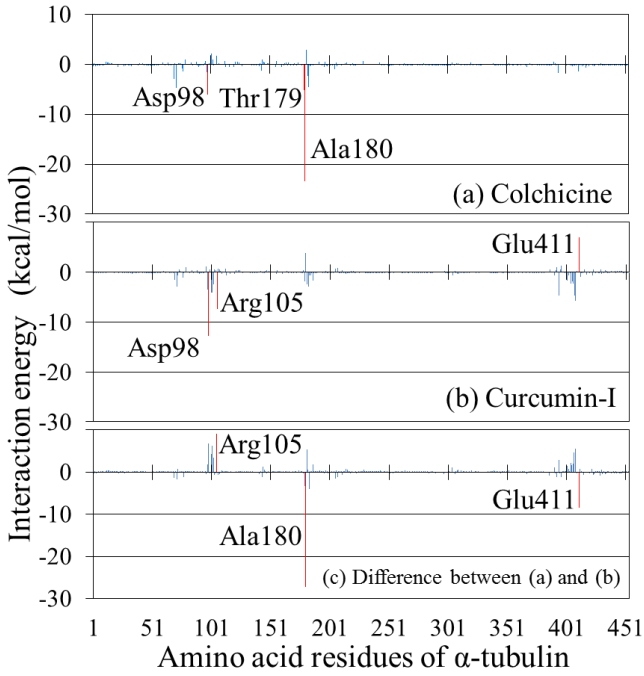

Figure 5. Interaction energies between amino acid residues of α-tubulin and ligand; (a) colchicine, (b) curcumin-I and (c) difference between (a) and (b)
Curcumin-I is docked to the colchicine site of α-tubulin.

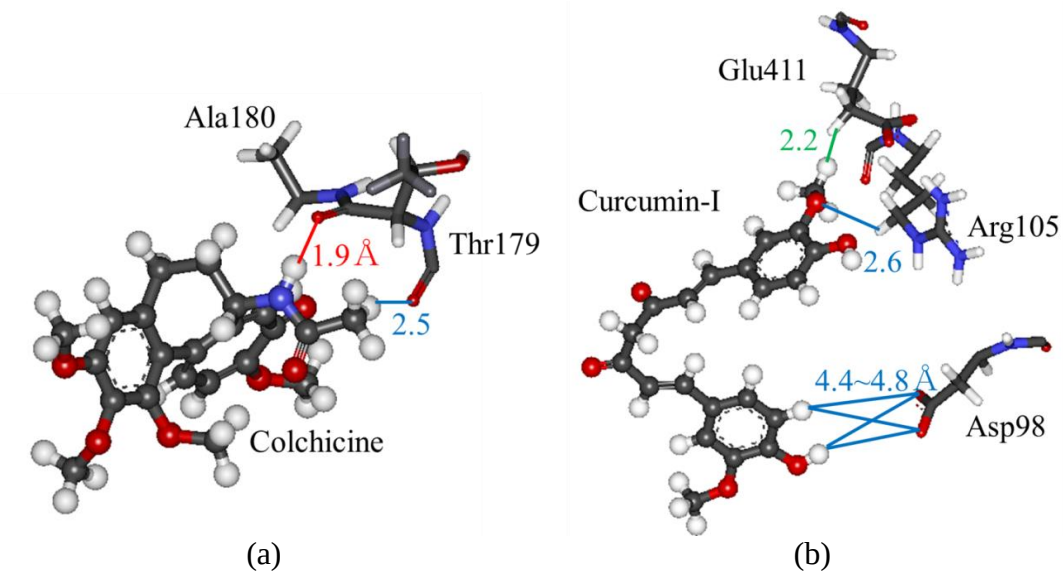

Figure 6. Interacting structures between some residues of α-tubulin; (a) colchicine and (b) curcumin-I at the colchicine-binding site
Red, blue and green lines indicate hydrogen-bonding, attractive electrostatic and repulsive interactions, respectively.

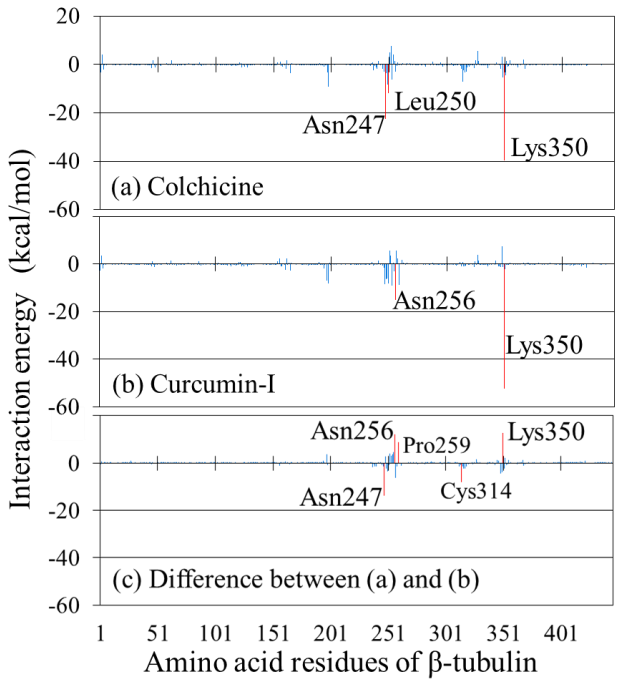

Figure 7. Interaction energies between amino acid residues of β-tubulin and ligand; (a) colchicine, (b) curcumin-I and (c) difference between (a) and (b)
Curcumin-I is docked to the colchicine binding-site of β-tubulin.

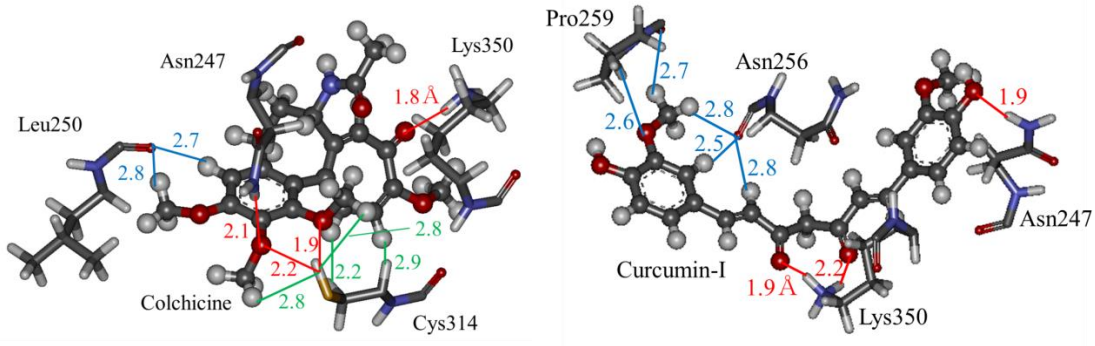

(a) (b)

Figure 8. Interacting structures between some residues of β-tubulin; (a) colchicine and (b) curcumin-I at the colchicine-binding site
Red, blue and green lines indicate hydrogen-bonding, attractive electrostatic and repulsive interactions, respectively.

3.2. Specific interactions between tubulin and curcumin-I at some binding sites

By use of AutoDock4.2 [17], 250 candidate poses of curcumin-I docked to α- or β-tubulin were created, and they were grouped into clusters based on the similarity of the docked structures. As the docking site of curcumin-I, we considered both the vinblastine-binding and the colchicine-binding sites. The number of clusters created by AutoDock4.2 are 51 (for the vinblastine-binding site of α-tubulin), 75 (for the vinblastine-binding site of β-tubulin), 66 (for the colchicine-binding site of α-tubulin) and 48 (for the colchicine-binding site of β-tubulin). Among these clusters, the top three ranked clusters with a number of poses larger than 10 were selected, and their representative structures were employed as the candidate structures for the tubulin+curcumin-I complexes. All candidate structures were fully optimized in explicit water by the classical AMBER-MM method as described in Section 2.

We first investigated the interactions between α-tubulin and curcumin-I at the vinblastine-binding site, using the FMO method. Table 1 lists the total energies (TEs) relative to that of the most stable structure of the tubulin+curcumin-I complex. For the α-tubulin+curcumin-I docked at the vinblastine-binding site, the 92nd pose is the most stable, and the other poses are at least 24.3 kcal/mol less stable than the 92nd pose. Therefore, we considered the 92nd pose as one of the stable structures for the α-tubulin+curcumin-I complex. To estimate the binding affinity between α-tubulin and curcumin-I, we evaluated the BE between them. The result is compared with that of vinblastine in Table 2. The BE for curcumin-I is larger than that for vinblastine, indicating the possibility of curcumin-I as a potent ligand to α-tubulin. In order to make clear the difference in binding properties of vinblastine and curcumin-I, we furthermore analyzed the IFIE between each amino acid residue of α-tubulin and curcumin-I. In Figure 2, the result for curcumin-I is compared with that for vinblastine. Curcumin-I interacts most strongly with Leu248 and additionally with Asn329 and Gly354. The interaction between curcumin-I and Leu248 is the main reason for the larger BE for curcumin-I. The interacting structure between α-tubulin and curcumin-I is shown in Figure 9(a), indicating a strong hydrogen bond between Leu248 and curcumin-I. In addition, there are some electrostatic interactions between curcumin-I and Asn329 and Gly354 residues.

Table 1. Total energy (TEs; kcal/mol) relative to that of the most stable structure for tubulin+curcumin-I complexes at the two docking sites; the number indicates the number of the pose created by AutoDock
Curcumin-I was docked to the vinblastine or the colchicine binding site of the α- and the β-tubulins.

	α-tubulin		β-tubulin	
Docking site	No.	ΔTE	No.	ΔTE
Vinblastine	92	0.0	11	0.0
	94	24.3	147	113.7
	120	39.3	191	111.9
Colchicine	97	15.7	145	31.6
	154	0.0	196	20.0
	238	215.9	227	0.0

Table 2. Binding energies (kcal/mol) between tubulin and ligand (curcumin-I, vinblastine and colchicine) evaluated by *ab initio* FMO method
curcumin-I was docked to the vinblastine or the colchicine binding site of tubulin.

Docking site	Ligand	α-tubulin	β-tubulin
Vinblastine	Curcumin-I	51.5	68.4
	Vinblastine	48.2	37.4
Colchicine	Curcumin-I	34.7	88.1
	Colchicine	36.8	93.0

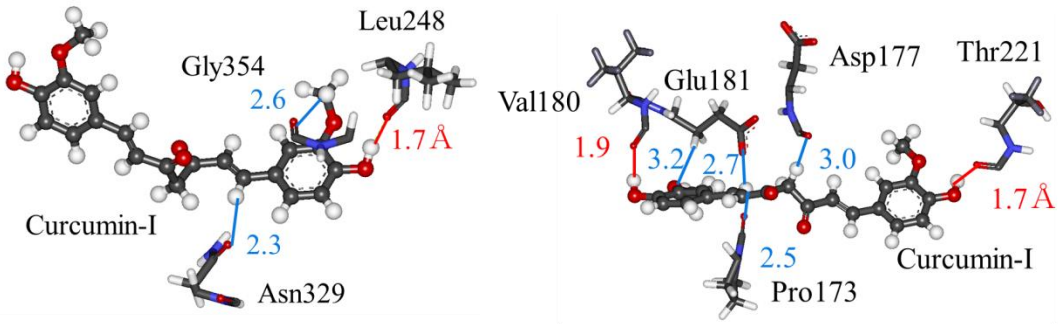

(a) (b)

Figure 9. Interacting structures between curcumin-I and some tubulin residues; (a) α-tubulin and (b) β-tubulin at the vinblastine binding-site
Red and blue lines indicate hydrogen-bonding and electrostatic interactions, respectively.

Next, we investigated the interactions between β-tubulin and curcumin-I at the vinblastine-binding site. As shown in Table 1, the 11th structure of β-tubulin+curcumin-I complex is at least 112 kcal/mol stable than the other clusters. Therefore, we select this structure as the most stable one of the β-tubulin+curcumin-I complex. As listed in Table 2, the BE between β-tubulin and curcumin-I is 31 kcal/mol larger than that for vinblastine. It is thus expected that curcumin-I acts as a potent ligand for *Plasmodium* β-tubulin. The IFIEs between β-tubulin and curcumin-I are shown in Figure 4(b), indicating that curcumin-I has the strongest attractive interaction with Glu181. In addition, curcumin-I interacts strongly with the Pro173, Asp177, Val180 and Thr221 of β-tubulin. The interacting structure between these residues and curcumin-I are shown in Figure 9(b), which elucidates the strong hydrogen bonds between the hydroxyl groups existing at the both ends of curcumin-I and Thr221 or Val180. Additionally, Pro173, Asp177 and Glu181 can interact electrostatically with curcumin-I. Since the central part of curcumin-I has no significant contribution to the binding between curcumin-I and β-tubulin as shown in Figure 9(b), it is expected that the introduction of some groups into the central part can enhance the interaction between curcumin-I and some residues of β-tubulin.

To search for the other binding site of curcumin-I to α-tubulin, we docked curcumin-I at the colchicine-binding site of α-tubulin and investigated its potential binding in this site. As listed in Table 1, the 154th pose of the α-tubulin+curcumin-I complex model created by AutoDock is the most stable among the top ranked three poses. For this structure, the BE between α-tubulin and curcumin-I was evaluated. As listed in Table 2, the BE of curcumin-I at the colchicine site is smaller than that of colchicine. We furthermore investigated the IFIEs between α-tubulin residues and curcumin-I and compared it with the IFIEs for colchicine. As shown in Figure 5(a), colchicine has strong attractive interaction with Ala180 and additional interactions with Asp98 and Thr179. In contrast, curcumin-I interacts attractively with Asp98 and Arg105 and interacts repulsively with Glu441. It is therefore elucidated that the binding mode of curcumin-I to the colchicine-binding site of α-tubulin is significantly different from that of colchicine. In particular, the interaction with Ala180 of α-tubulin is significantly different for colchicine and curcumin-I, as shown in Figure 5(c). To make clear the reason for this difference, we analyzed the interacting structures between these residues and colchicine or curcumin-I. As shown in Figure 6, colchicine interacts with the backbone oxygen atoms of Thr179 and Ala180, while curcumin-I interacts with Arg105 and Asp98. It is noted that Glu441 and curcumin-I interact repulsively at 2.2 Å distance. As a result, the IFIE between curcumin-I and Glu441 becomes positive, as shown in Figure 5(b). By introducing some group into the terminal part of curcumin-I, it is expected that the repulsive interaction will be reduced, resulting in larger BE between α-tubulin and curcumin-I.

Finally, we investigated the specific interactions between β-tubulin and curcumin-I at the colchicine-binding site, in order to clarify the differences in curcumin and colchicine bindings with β-tubulin. As listed in Table 1, the 227th pose of the β-tubulin+curcumin-I complex is the most stable. The BE between β-tubulin and curcumin-I (88.1 kcal/mol) is smaller than that (93.0 kcal/mol) of colchicine, as listed in Table 2. Therefore, in comparison with colchicine, curcumin-I has weak binding to β-tubulin. The IFIEs between β-tubulin residues and ligand are compared in Figure 7. Both ligands are demonstrated to have strong attractive interaction with Lys350. In addition, colchicine interacts with Asn247 and Leu250, while curcumin-I interacts with Asn256. The interacting structures between these residues and ligands are compared in Figure 8. Colchicine forms hydrogen bonds with Lys350 and Cys314, while curcumin-I forms two hydrogen bonds with Lys350 and a hydrogen bond with Asn247. Due to these bonds, we assume that curcumin-I has stronger attractive interaction with Lys350 than colchicine.

3.3 Comparison of tubulin binding with curcumin-I and canonical drugs

To predict the binding affinity between α- or β-tubulin and ligand, we investigated their BEs, under the assumption that the entropic effect on binding affinity is the same for the ligands, because a vibrational analysis for the tubulin+ligand complex is not practical via the *ab initio* FMO method. As listed in Table 2, the BEs between β-tubulin and curcumin-I as well as colchicine are remarkably larger than those for the other ligand and tubulin. It is thus concluded that curcumin-I as well as colchicine bind strongly to β-tubulin to be a potent inhibitor of β-tubulin. Furthermore, it is indicated in Figure 8(b) that the hydrogen atoms existing at the central part of curcumin-I has no significant contribution to the interaction with the β-tubulin. Therefore, it is expected that the introduction of some substituted groups in the central part of curcumin-I enhances the binding affinity between curcumin-I and β-tubulin.

According to the results of our study (see Table 2), curcumin-I prefers to bind in the colchicine site of β-tubulin and the vinblastine site of α-tubulin. This indicates that curcumin-I has both functions of vinblastine and colchicine at the different binding-sites of the α- and β-tubulins. Table 2 also indicates that curcumin-I has larger BEs for the both tubulins than vinblastine. It is thus expected that curcumin-I has more significant effect on these tubulins than vinblastine. In this way, curcumin derivatives can be considered as promising inhibitors against the formation of microtubules, acting as on α/β-tubulin heterodimer formation, as well as on formation of microtubule protofilament in *Plasmodium* species [29].

4. Conclusions

In the present study, the specific interactions between α- or β-tubulin and ligand were investigated, using molecular-docking, MM optimization and *ab initio* FMO calculations. The results for the existing drugs (vinblastine and colchicine) as well as natural agent curcumin-I elucidate the following points.

(1) *Ab initio* FMO calculations confirmed the experimental data on the inhibitory effect of curcumin-I on malaria parasites and showed that this effect can be realized through its direct binding with α- and β-tubulins.

(2) Anti-microtubule effect of curcumin-I may come from its vinblastin-specific site binding with α- and β-tubulins.

(3) Curcumin-I and colchicine bind more strongly to β-tubulin rather than α-tubulin, mainly due to their strong interactions with Lys350 of β-tubulin.

(4) Taking into account the topology of colchicine and vinblastin sites, curcumin derivatives can be considered as promising inhibitors of microtubule-formation, disturbing α/β-tubulin heterodimer and microtubule protofilament formation in *Plasmodium* species.

Acknowledgements

This study was supported by the international internship program of Japan Student Services Organization (JASSO), the student exchange program between the Institute for Food Biotechnology

and Genomics of the National Academy of Sciences of Ukraine and Toyohashi University of Technology, and the JSPS Grant-in-Aid for Challenging Exploratory Research (No. 22650061) between Toyohashi University of Technology and the three institutes of the National Academy of Science of Ukraine.

References

[1] World Health Organization, *World Malaria Report 2017*.
[2] Maheshwari, R. K.; Singh, A. K.; Gaddipati, J.; Srimal, R. C. Multiple biological activities of curcumin: a short review. *Life Sci.* **2006**, *78*, 2081-2087.
[3] Cui, L.; Miao, J.; Cui, L. Cytotoxic effect of curcumin on malaria parasite plasmodium falciparum: inhibition of histone acetylation and generation of reactive oxygen species. *Antimicrob. Agents Chemother*. **2007**, *51*, 488-494.
[4] Nandakumar, D. N.; Nagaraj, V. A.; Vathsala, P. G.; Rangarajan, P.; Padmanaban, G. Curcumin artemisinin combination therapy for malaria. *Antimicrob. Agents Chemother.* **2006**, *50*, 1859-1860.
[5] Reddy, R. C.; Vatsala, P. G.; Keshamouni, V. G.; Padmanaban, G.; Rangarajan, P. N. Curcumin for malaria therapy. *Biochem. Biophys. Res. Commun.* **2005**, *326*, 472-474.
[6] Van Erk, M. J.; Teuling, E.; Staal, Y. C.; Huybers, S.; Van Bladeren, P.J.; *et al.* Time- and dose-dependent effects of curcumin on gene expression in human colon cancer cells. *J. Carcinog.* **2004**, *3*, 8 (17 pages).
[7] Gupta, K. K.; Bharne, S. S.; Rathinasamy, K.; Naik, N. R.; Panda, D. Dietary antioxidant curcumin inhibits microtubule assembly through tubulin binding. *FEBS J.* **2006**, *273*, 5320-5332.
[8] Chakrabarti, R.; Rawat, P. S.; Cooke, B. M.; Coppel, R. L.; Patankar, S. Cellular effects of curcumin on plasmodium falciparum include disruption of microtubules. *PLoS ONE* **2013**, *8*, e57302 (14pages).
[9] Gigant, B.; Wang, C.; Ravelli, R. B. G.; Roussi, F.; Steinmetz, M. O.; *et al*. Structural basis for the regulation of tubulin by vinblastine. *Nature* **2005**, *435*, 519-522.
[10] Ravelli, R. B. G.; Gigant, B.; Curmi, P. A.; Jourdain, I.; Lachkar, S.; *et al*. Insight into tubulin regulation from a complex with colchicine and a stathmin-like domain. *Nature* **2004**, *428*, 198-202.
[11] Roy, A.; Kucukural, A.; Zhang, Y. I-TASSER: a unified platform for automated protein structure and function prediction. *Nat. Protoc.* **2010**, *5*, 725-738.
[12] Roy, A.; Yang, J.; Zhang, Y. COFACTOR: an accurate comparative algorithm for structure-based protein function annotation. *Nucleic Acids Res.* **2012**, *40*, 471-477.
[13] Li, H.; Robertson, A. D.; Jensen, J. H. Very fast empirical prediction and rationalization of protein pKa values. *Proteins* **2005**, *61*, 704-721.
[14] Bas, D. C.; Rogers, D. M.; Jensen, J. H. Very fast prediction and rationalization of pKa values for protein and ligand complexes. *Proteins* **2008**, *73*, 765-783.
[15] Frisch, M. J.; *et al. Gaussian 09*. Revision A.02, Gaussian, Inc., Wallingford CT, 2009.
[16] Besler, B. H.; Merz Jr. K. M.; Kollman, P. A. Atomic charges derived from semiempirical methods. *J. Comput. Chem.* **1990**, *11*, 431-439.
[17] Morris, G. M.; Huey, R.; Lindstrom, W.; Sanner, M. F.; Belew, R. K.; *et al*. Autodock4 and AutoDockTools4: automated docking with selective receptor flexibility. *J. Comput. Chem.* **2009**, *30*, 2785-2791.
[18] Case, D. A.; *et al. AMBER 12*. University of California, San Francisco, 2012.

[19] Lindorff-Larsen, K.; Piana, S.; Palmo, K.; Maragakis, P.; Klepeis, J. L.; *et al.* Improved side-chain torsion potentials for the Amber ff99SB protein force field. *Protein* **2010**, *78*, 1950-1958.
[20] Jorgensen, W. L.; Chandrasekhar, J.; Madura, J. D.; Impey, R. W.; Klein, M. L. Comparison of simple potential functions for simulating liquid water. *J. Chem. Phys*. **1983**, *79*, 926-935.
[21] Wang, J.; Wolf, R. M.; Caldwell, J. W.; Kollman, P. A.; Case, D. A. Development and testing of a general amber force field. *J. Comput. Chem.* **2004**, *25*, 1157-1174.
[22] Kitaura, K.; Ikeo, E.; Asada, T.; Nakano, T.; Uebayashi, M. Fragment molecular orbital method: an approximate computational method for large molecules. *Chem. Phys. Lett.* **1999**, *313*, 701-706.
[23] Tanaka, S.; Mochizuki, Y.; Komeiji, Y.; Okiyama, Y.; Fukuzawa, K. Electron-correlated fragment-molecular-orbital calculations for biomolecular and nano systems. *Phys. Chem. Chem. Phys.* **2014**, *16*, 10310-10344.
[24] Mochizuki, Y.; Yamashita, K.; Nakano, T.; Okiyama, Y.; Fukuzawa, K.; *et al*. Higher-order correlated calculations based on fragment molecular orbital scheme. *Theor. Chem. Acc*. **2011**, *130*, 515-530.
[25] Mochizuki, Y.; Koikegami, S.; Nakano, T.; Amari, S.; Kitaura, K. Large scale MP2 calculations with fragment molecular orbital scheme. *Chem, Phys. Lett.* **2004**, *396*, 473-479.
[26] Mochizuki, Y.; Nakano, T.; Koikegami, S.; Tanimori, S.; Abe, Y.; *et al.* A parallelized integral-direct second-order Mφller-Plesset perturbation theory method with a fragment molecular orbital scheme. *Theor. Chem. Acc.* **2004**, *112*, 442-452.
[27] Ranaivoson, F. M.; Gigant, B.; Berritt, S.; Joullie, M.; Knossow, M. Structural plasticity of tubulin assembly probed by vinca-domain ligands. *Acta Crystallogr. D* **2012**, *68*, 927-934.
[28] Prota, A. E.; Danel, F.; Bachmann, F.; Bargsten, K.; Buey, R. M.; *et al*. The novel microtubule-destabilizing drug BAL27862 binds to the colchicine site of tubulin with distinct effects on microtubule organization. *J. Mol. Biol.* **2014**, *426*, 1848-1860.
[29] Field, J. J.; Waight, A. B.; Senter, P. D. A previously undescribed tubulin binder. *Proc. Natl. Acad. Sci. U.S.A.* **2014**, *111*, 13684-13685.